GeoConvention 2015
GEOSCIENCE
new horizons
Telus Convention Centre • 4-8 May 2015 • Calgary, AB Canada

Effects of Finite Specimen Dimensions on Laboratory Measurements of Rock Moduli and Q

Wubing Deng and Igor B. Morozov
University of Saskatchewan

Summary

Laboratory measurements are viewed as a direct way to understand the physical properties of rocks, such as their compressional and shear moduli and parameters of anelasticity. The moduli, Q-factors and densities measured in the laboratory are commonly used to compare to the seismic-wave properties measured in the field and to develop fluid-substitution and effective-media models. However, in laboratory measurements, the resulting values of frequency-dependent moduli and Q may be affected by finite dimensions of the specimens. The general reason for this influence is that in a finite specimen, multiple wave modes are always present, whereas only a single, traveling wave is used in field observations. To examine these effects of specimen length, we consider theoretical models of three experiments with elastic, viscoelastic, and poroelastic rock, by using the common specimen lengths of 10 to 20 cm. The finite length of the cylindrical specimen causes a reduction in the measured P-wave modulus M at higher frequencies. For elastic rock, the values of M and the Q are close to those for a P-wave in the field. For a viscoelastic material with $Q \approx 100$, the values of higher-frequency M measured in the samples are significantly lower than the M measured from seismic wave velocities. For a poroelastic material such as fully-saturated sandstone, the drop in M in short samples occurs at much lower frequencies than the increase due to poroelastic effects. The increase of attenuation (Q^{-1}) within short samples also occurs at frequencies much lower and is much steeper than the peak in poroelastic dissipation. These effects should be particularly strong for materials with wave-induced flows (WIFF), in which the wavelengths of the slow and diffusive fluid-related waves can be comparable to the length of the specimen. In such cases, the effects of finite sample length may significantly complicate the observation of the pore-fluid related modulus dispersion and attenuation.

Introduction

Laboratory experiments on rocks or drill cores are considered as the most direct way for studying mechanical rock properties and seismic-wave propagation characteristics, such as the P-wave/S-wave moduli and seismic attenuation (Spencer 2013; Tisato et al. 2014). Spencer (2013) quantitatively analyzed the temperature and frequency dependence of velocities and attenuation by conducting experiments on 11-cm long samples of Ells River bitumen sands from Alberta, Canada. Tisato et al. (2014) collected a large amount of data on Berea sandstone to study the attenuation caused by wave-induced flows. In addition to laboratory experiments, numerical modelling was also utilized to explore seismic wave behaviour and rock properties in the lab (Rubino et al. 2009; Rubino and Holliger 2013, Tisato et al. 2014). Numerical modeling is a very good way to examine the proposed mathematical and physical descriptions of the subsurface rock (Murphy et al. 1986; Tisato et al. 2014).

The point of the present paper is that although this is rarely noted, the moduli and Q results obtained for short samples may not be automatically applicable to field observations at the same frequency. This observation applies to both laboratory experiments and their numerical models. There are two reasons for these differences in the moduli: 1) finite dimensions of the specimen and 2) the presence of

transverse deformations requiring transforming the observed Young's moduli into P-wave moduli. The first of these effects is considered in this study.

In subresonant laboratory measurements, the samples are normally much shorter than the seismic wavelengths. However, for longer samples of porous, fluid-saturated rock (as in Tisato et al. 2014) at the high-frequency end of the band, the length of the sample may become comparable to the wavelengths of Biot's slow P waves, and particularly of similar modes associated with wave-induced flows (WIFF) within the rock. In a finite rock sample under a dynamic loading experiment, multiple wave modes traveling in both directions are present, and the interference of these waves may result in measurements different from those in traveling waves in the field. In this paper, four numerical modelling experiments are undertaken to illustrate the effects of the finite sizes of the samples on the measurements of elastic moduli and Q.

Method

Consider a schematic experiment with axial loading of a cylindrical rock sample in the laboratory (Figure 1). The bottom of the specimen is fixed, and to the top, pressure p is applied. Note that the effective modulus M_{eff} measured in this experiment is not automatically a stress/strain ratio but a ratio of the applied pressure, p, to the *average* strain of the specimen:

$$M_{eff} = \frac{p}{u/L}, \tag{1}$$

where u the displacement of the upper end, and L is the length of the sample (Figure 1). This effective modulus M_{eff} is a constant when p is a static loading pressure. To study the frequency dependence of M_{eff}, and the corresponding attenuation Q, consider a dynamic loading pressure $p = p_0 e^{-i\omega t}$, where ω is the angular frequency. This pressure will generate a standing wave within the cylinder, consisting of two (for a viscoelastic material) or four (for the poroelastic case) several wave modes traveling in the upward and downward directions:

$$u_n(t,x) = A_n e^{-i(\omega t - k_n x)} \tag{2}$$

where $\mathbf{A}_n$ is the amplitude and $\boldsymbol{k}_n$ is the wavenumber of *n*-th mode, x is the distance along the sample, and *t* is the time. Let us denote the spatial dependence of u by $u_n(x) = A_n e^{ik_n x}$. From eq. (2), the spatial distribution of strain within each mode equals:

$$\varepsilon_n(x) = \frac{\partial u_n(x)}{\partial x} = ik_n A_n e^{ik_n x} \tag{3}$$

For each mode, the axial stress $\sigma_n(x)$ can be evaluated from its strain by using the appropriate viscoelastic or poroelastic equations. This relation can be expressed through a "modulus" M_n for the mode:

$$\sigma_n(x) = M_n \varepsilon_n(x) \tag{4}$$

From eq. (1) the measured effective modulus can be written as a superposition of stresses and displacements of the wave modes:

$$M_{eff} = L \frac{\sum_n M_n \varepsilon_n(L)}{\sum_n u_n(L)}. \tag{5}$$

Thus, the oserved empirical modulus is not a pure material property but an average of the moduli M_n for the wave modes weighted by the strains and displacements of these modes.

Model Experiments

In the following model experiments, we calculate the effective modulus in eq. (5) for four key types of materials. For simplicity, we consider a pure P-wave deformation case, in which all displacements occur along the axis of the cylinder.

Elastic Solid

Consider an elastic cylinder with a P-wave modulus M, which would the modulus measured as $M = \rho V_P^2$ in a P-wave in a bound less medium. Within a finite cylinder, a standing wave is formed consisting of a wave traveling downward with amplitude that we denote $\underset{\leftarrow}{A}$ and another wave traveling upward, with amplitude $\underset{\rightarrow}{A}$. The moduli M_n for both of these waves equal M. Since the bottom of the cylinder is fixed, these amplitudes are related by $\underset{\rightarrow}{A} = -\underset{\leftarrow}{A}$. From eqs. (3) and (5), we therefore have:

$$M_{eff} = MkL\cot\left(kL\right) \tag{6},$$

where k is the wavenumber. For a short cylinder, $kL \ll 1$, and we can use a Taylor-series approximation:

$$\frac{M_{eff}}{M} \approx 1 - \frac{\left(kL\right)^2}{3}. \tag{7}.$$

Figure 2 shows the variation of this ratio with frequency and specimen length L. The effective modulus M_{eff} is approximately equal M at low frequencies, with an approximately 2% drop at 1 kHz. At frequencies above 1 kHz, the modulus drops sharply. The frequencies at which the drop in M_{eff}/M occurs are inversely proportional to the length of the specimen.

Viscoelastic Solid

For a viscoelastic material, the wave mode content and boundary conditions are the same as for an elastic solid. Therefore, eq. (6) remains valid, with both moduli M and M_{eff} becoming complex-valued.

In this experiment, we construct a viscoelastic solid model with a near-constant $Q \approx 100$ by using five Maxwell-solids (Figure 3). Both moduli and attenuation factors are in a good agreement below about 1 kHz. At higher-frequencies, the values of M_{eff} measured in the samples are significantly lower than the M measured from seismic wave velocities. At the same time the bias in the inverse Q due to the finite length of the sample is small (Figure 3).

Poroelastic Solid

In contrast to the cases of elastic and viscoelastic materials, four P waves are excited in a poroelastic cylinder: the fast P-wave Biot slow P-wave traveling upward and similar waves travelling downward. In this experiment, additional boundary conditions are required for fluid flow; we consider the case of impermeable (jacketed) boundaries on all sides of the cylinder.

By evaluating expressions (2), (3), and (5) for sandstone in Biot's poroelasticity, we obtain the short-sample effective modulus shown in Figure 4. In this case, the modulus of the primary P wave is taken as the traveling-wave modulus *M*. Within the seismic frequency band, the moduli M and M_{eff} agree with each other. Above about 1 kHz, the effective modulus drops sharply. Note that the attenuation peak in a poroelastic media commonly occurs in the ultrasonic frequency band; however, the effect of finite sample size occurs at much lower frequencies (Figure 4).

Poroelastic Solid With Squirt Flow

Squirt flows and WIFF are is considered the major cause of attenuation within the seismic sonic-log frequency bands (Rubino and Holliger, 2013). Similarly to the poroelastic case, four P waves are excited within the cylinder, and the boundary conditions are also the same as in the poroelastic case. However, an additional, lower-frequency attenuation peak appears in the primary-wave attenuation (Figure 5). This peak around 100 Hz is due to squirt flows. The effect of the finite size of the specimen again leads to the measured modulus dropping and the attenuation increasing above about 1 kHz.

Conclusions

The differences between the effective elastic moduli and Q measured in the lab and in the field are examined by numerical modeling. For an elastic material, the discrepancy is small, with only 2-3% difference for typical sample sizes and within the seismic frequency band. For a viscoelastic material, the difference is increased, so that the dispersion curve for the effective modulus does not reach the unrelaxed modulus measured in the field. For poroelastic rock with squirt flows and WIFF, the difference between the lab and field moduli is further increased, particularly by the effects of diffusive slow waves within the finite specimen.

Acknowledgements

This study was supported by P. R. China Scholarship Council.

References

Murphy, W. F., K. W. Winkler, and R. L. Kleinberg, 1986, Acoustic relaxation in sedimentary rocks, dependence on grain contacts and fluid saturation: Geophysics, 51, 757–766.

Rubino, J. G., and Holliger, K., 2013, Research note: Seismic attenuation due to wave-induced fluid flow at microscopic and mesoscopic scales: Geophysical Prospecting, 61, 882-889.

Rubino, J G., Ravazzoli, C. L., and Santos, J. E., 2009, Equivalent viscoelastic solids for heterogeneous fluid-saturated porous rocks: Geophysics, 74(1), N1-N13.

Spencer, J. W., 2013, Viscoelasticity of Ells River bitumen sand and 4D monitoring of thermal enhanced oil recovery processes: Geophysics, 78(6), D419-D428.

Tisato, N., Quintal, B., Chapman, S., Madonna, C., Subramaniyan, S., Frehner, M., Saenger, E. H. and Grasselli, G., 2014, Seismic attenuation in partially saturated rocks: Recent advances and future directions: The Leading Edge, 33(6), 640-646.

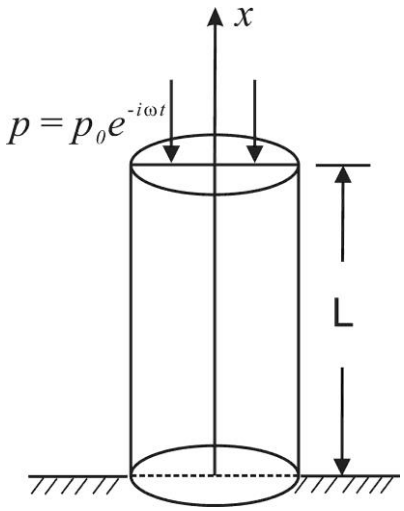

Figure 1. Schematic model for the three numerical experiments with rock samples in the lab.

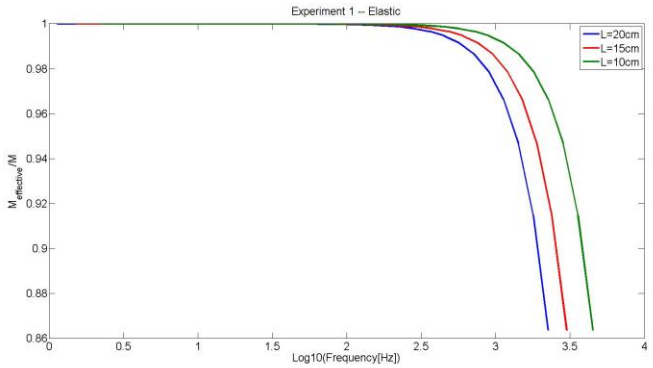

Figure 2. Frequency dependence of the effective modulus in an elastic cylinder of length *L*.

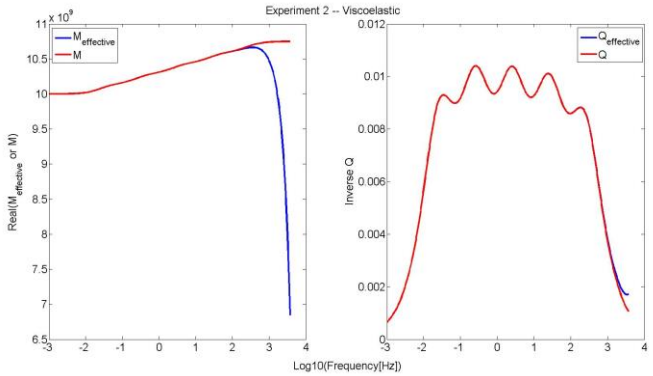

Figure 3. Effective modulus (left) and attenuation variation (right) in a viscoelastic cylinder. Red lines are dependences for unbounded media, red lines – for a cylinder of 11-cm length.

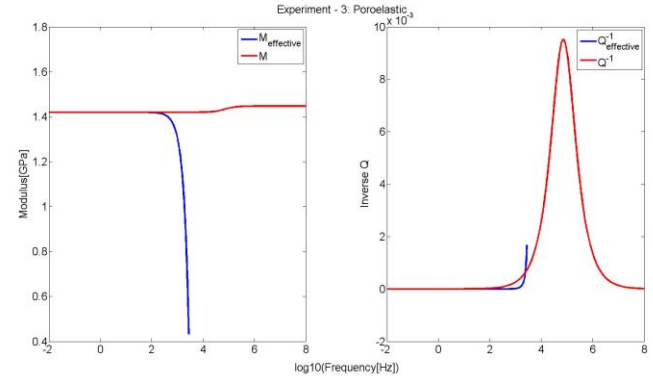

Figure 4. Models of effective modulus (left) and attenuation (right) measured in a poroelastic cylinder.

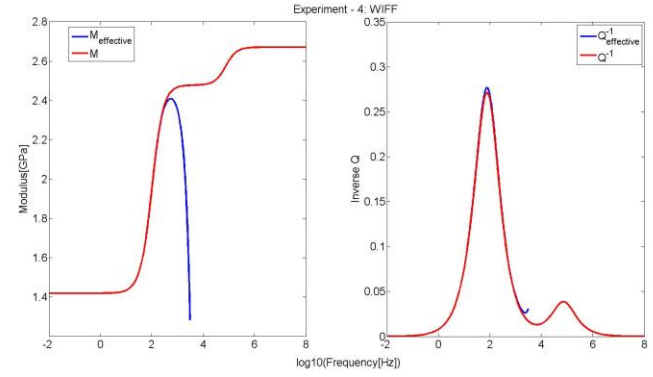

Figure 4. Models of effective modulus (left) and attenuation (right) measured in poroelastic solid with squirt flow.